Adaptive and Robust Linearizing Control Strategies for Fed-Batch Cultures of Microorganisms Exhibiting Overflow Metabolism

Laurent Dewasme[1,⋆], Daniel Coutinho[2], and Alain Vande Wouwer[1]

[1] Automatic Laboratory, Faculty of Engineering of the University of Mons
Boulevard Dolez, 31, 7000 Mons, Belgium
[2] Department of Automation and Systems, Federal University of Santa Catarina
476 Florianopolis, 88040-900, Brazil
{Laurent.Dewasme,Alain.VandeWouwer}@umons.ac.be,
Coutinho@das.ufsc.br

Abstract. Linearizing control is a popular approach to control bioprocesses, which has received considerable attention is the past several years. This control approach is however quite sensitive to modeling uncertainties, thus requiring some on-line parametric adaptation so as to ensure performance. In this study, this usual adaptive strategy is compared in terms of implementation and performance to a robust strategy, where the controller has a fixed parametrization which is determined using the LMI framework so as to ensure robust stability and performance. Fed-batch cultures of yeast and bacteria are considered as application examples.

Keywords: Nonlinear robust control, Adaptive Control, Fermentation Process, Biotechnology.

1 Introduction

1.1 Context and Motivation

The culture of host recombinant microorganisms is nowadays a very important way of producing biopharmaceuticals. Fed-batch operation is popular in industrial practice since it is advantageous from an operational point of view to feed the cells (also called biomass) progressively as they grow, instead of overfeeding the bioreactor, which can inhibit the cell growth. The off-line determination of the feeding profile is usually suboptimal as some security margin has to be provided in order to avoid this possible excess of substrate leading to the accumulation of inhibitory byproducts (inhibition of the cell respiratory capacity), namely ethanol for yeast cultures and acetate for bacteria cultures. To optimize the culture conditions and to avoid high concentrations of inhibitory byproducts, a closed-loop solution is required, and a wide diversity of approaches, e.g., [1], [11], [4], [13], [12], [7], [18], [8] have been considered.

⋆ This paper presents research results of the Belgian Network DYSCO (Dynamical Systems, Control, and Optimization), funded by the Interuniversity Attraction Poles Program, initiated by the Belgian State, Science Policy Office. The scientific responsibility rests with its authors.

J.A. Cetto et al. (Eds.): Informatics in Control, Automation and Robotics, LNEE 89, pp. 283–305.
springerlink.com

As discussed in [4], several control strategies can be applied to define an optimal feeding profile (usually considered as the sole manipulated variable in most of the published studies). In order to maintain the system in optimal conditions, it is possible to control the RQ (respiratory coefficient) of the cells using gas analyzer measurements, to keep the system at a very low critical substrate concentration, or to control the byproduct concentration at a sufficiently low level.

For example, in [18] and [8], two extremum-seeking strategies regulating the substrate level around the optimal critical value are investigated. This kind of approach can however only be applied when this critical value is measurable, which is generally difficult for yeasts and bacteria cultures considering the sensitivity of the probes currently available on the market.

In [1], a classical PID with gain scheduling is used to control the byproduct concentration. However, this investigation shows that a PID controller is unable to track an exponential trajectory as small tracking errors evolves exponentially.

In [12] and [7], a robust linear controller is applied to regulate the byproduct concentration. The main advantage of this controller is to require minimum a priori knowledge, i.e. one yield coefficient and the measurement of the byproduct concentration.

Among the published studies, linearizing control [2] is a very popular approach, which has been applied succesfully in a number of case studies (see [11],[4],[13]). However, linearizing control is by essence model-based and, therefore, requires the knowledge of an accurate model. As bioprocess models are generally uncertain, adaptation is required using observer-based or least-squares strategies. Whereas parametric adaptation is a simple approach, it does not guarantee stability in the presence of unmodeled dynamics or too high noise levels.

In this paper, another approach is considered, which is based on nonlinear robust control and the use of Linear Matrix Inequalities (LMIs) to design the free linear dynamics so as to ensure robust stability and performance in presence of model uncertainties. A comparison of the adpative and robust control approaches is provided in terms of implementation, and simulation tests show the respective advantages and limitations of both strategies.

2 Model and Control Objectives

2.1 Model Description

In this section, we first consider a generic mechanistic model that would, in principle, allow the representation of the culture of different strains presenting an overflow metabolism (yeasts, bacteria, animal cells, etc).

This model describes therefore the cell catabolism through the following three main reactions:

$$\text{Substrate oxidation :} \quad k_{S1}\mathrm{S} + k_{O1}\,\mathrm{O} \overset{r_1 X}{\rightarrow} k_{X1}\,\mathrm{X} + k_{C1}\,\mathrm{C} \tag{1a}$$

$$\text{Substrate fermentation :} \quad k_{S2}\mathrm{S} + k_{O2}\,\mathrm{O} \overset{r_2 X}{\rightarrow} k_{X2}\,\mathrm{X} + k_{P2}\,\mathrm{P} + k_{C2}\,\mathrm{C} \tag{1b}$$

$$\text{Byproduct oxidation :} \quad k_{P3}\mathrm{P} + k_{O3}\,\mathrm{O} \overset{r_3 X}{\rightarrow} k_{X3}\,\mathrm{X} + k_{C3}\,\mathrm{C} \tag{1c}$$

where X, S, P, O and C are, respectively, the concentration in the culture medium of biomass, substrate (typically glucose), byproduct (i.e. ethanol or methanol in yeast cultures, acetate in bacteria cultures or lactate in animal cells cultures), dissolved oxygen and carbon dioxide. $k_{\xi i}$ ($i = 1, 2, 3$, $\xi =$ X, S, P, O, C) are the yield coefficients and r_1, r_2 and r_3 are the nonlinear specific consumption rates given by:

$$r_1 = \frac{\min\left(r_S, r_{S_{crit}}\right)}{k_{S1}} \tag{2a}$$

$$r_2 = \frac{\max\left(0, r_S - r_{S_{crit}}\right)}{k_{S2}} \tag{2b}$$

$$r_3 = \frac{\max\left(0, \frac{k_{os}(r_{S_{crit}} - r_S)}{k_{op}} \frac{P}{P+K_P}\right)}{k_{P3}} \tag{2c}$$

Note that these specific consumption rates are divided, for each reaction, by the corresponding substrate yield coefficient (k_{S1} and k_{S2} for the main substrate, usually glucose, in the first two reactions and k_{P3} for the substitute carbon source, the byproduct, in the third reaction) in order to normalize the consumption mechanism with respect to the substrate source. For instance, the substrate consumption rate of the first reaction is $k_{S1}r_1$ which is equal to r_S or $r_{S_{crit}}$ if the oxidative capacity is completely exploited, while the corresponding biomass growth rate is $k_{X1}r_1$ which is respectively equal to $\frac{k_{X1}}{k_{S1}}r_S$ or $\frac{k_{X1}}{k_{S1}}r_{S_{crit}}$. The yield coefficient ratio $\frac{k_{X1}}{k_{S1}}$ illustrates this normalization of the growth rate with respect to the substrate consumption. The kinetic terms associated with the substrate consumption r_S and the critical substrate consumption $r_{S_{crit}}$ (function of the cells oxidative or respiratory capacity r_O) are given by:

$$r_S = \mu_S \frac{\mathrm{S}}{\mathrm{S} + K_S} \tag{3a}$$

$$r_{S_{crit}} = \frac{r_O}{k_{os}} = \frac{\mu_O}{k_{os}} \frac{\mathrm{O}}{\mathrm{O} + K_O} \frac{K_{iP}}{K_{iP} + P} \tag{3b}$$

These expressions take the classical form of Monod laws where μ_S and μ_O are the maximal values of specific growth rates, K_S and K_O are the saturation constants of the corresponding element, and K_{iP} is the inhibition constant. k_{os} and k_{op} represent the coefficients characterizing respectively the yield between the oxygen and substrate consumptions, and the yield between the byproduct and oxygen consumptions. In order to illustrate the role of k_{os} and k_{op}, consider for instance the oxygen consumed in the first two reactions (1a) and (1b). As shown by Fig. 1, a certain substrate quantity equal to $k_{S1}r_1$ is oxidized using an equivalent oxygen quantity $k_{O1}r_{O1} = k_{S1}r_1$ where r_{O1} can be seen as the oxygen consumption rate in the first reaction. In a similar way, the equivalent substrate and oxygen quantities required by the second reaction are equal and respectively defined as $k_{S2}r_2$ and $k_{O2}r_{O2}$ where r_{O2} is the oxygen consumption rate in the second reaction. In order to link r_S to r_O, a global yield coefficient k_{os} is defined as $r_O = k_{os}r_S$. The introduction of k_{op} in the model follows therefore the same reasoning for the byproduct. Nevertheless, note that for particular cells which do not need oxygen in (1b), k_{os} is sometimes summarized to k_{O1} and, for analogous reasons, k_{op} to k_{O3}. As our aim is to provide a general representation of overflow metabolism, this notation is used in the following sections.

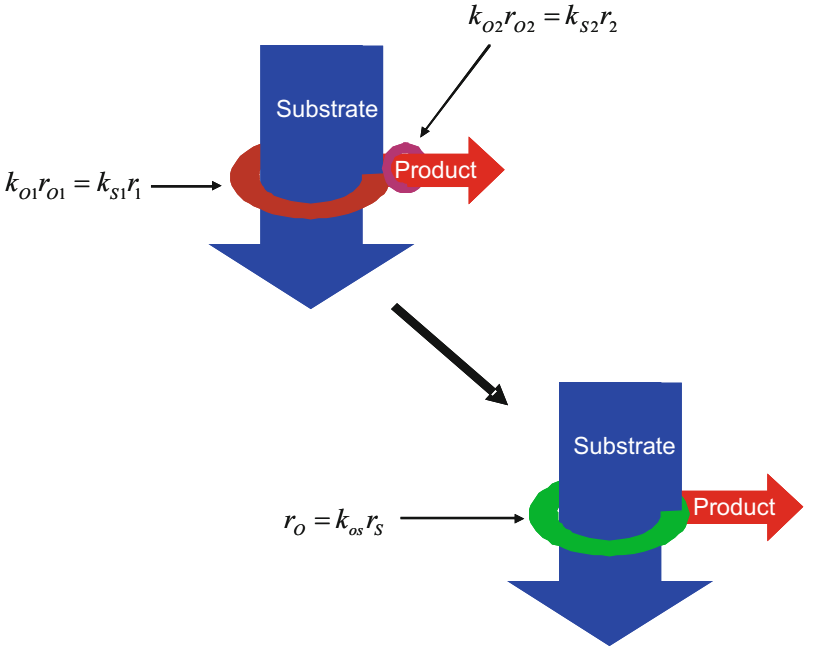

Fig. 1. Schematic representation of the simplified kinetic model using k_{os} as a global yield coefficient between the substrate and the oxygen consumptions

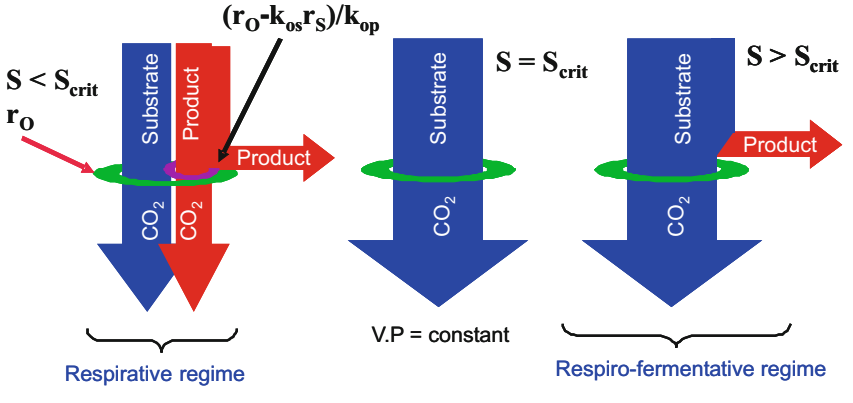

Fig. 2. Illustration of Sonnleitner's bottleneck assumption ([16]) for cells limited respiratory capacity

Kinetic model (2) is based on Sonnleitner's bottleneck assumption ([16]) which was applied to a yeast strain *Saccharomyces cerevisiae* (Figure 2). This model explains that during a culture, the cells are likely to change their metabolism because of their limited oxidative capacity. When the substrate is in excess (concentration $S > S_{crit}$ and the glucose consumption rate $r_S > r_{S_{crit}}$), the cells produce a byproduct P through the fermentative pathway, and the culture is said in (respiro-) fermentative (RF) regime.

On the other hand, when the substrate becomes limiting (concentration $S < S_{crit}$ and the glucose consumption rate $r_S < r_{S_{crit}}$), the available substrate (typically glucose), and possibly the byproduct P (as a substitute carbon source), if present in the culture medium, are oxidized. The culture is then said in respirative (R) regime.

Component-wise mass balances give the following differential equations:

$$\frac{dX}{dt} = (k_{X1}r_1 + k_{X2}r_2 + k_{X3}r_3)X - DX \tag{4a}$$

$$\frac{dS}{dt} = -(k_{S1}r_1 + k_{S2}r_2)X + DS_{in} - DS \tag{4b}$$

$$\frac{dP}{dt} = (k_{P2}r_2 - k_{P3}r_3)X - DP \tag{4c}$$

$$\frac{dO}{dt} = -(k_{O1}r_1 + k_{O2}r_2 + k_{O3}r_3)X - DO + OTR \tag{4d}$$

$$\frac{dC}{dt} = (k_{C1}r_1 + k_{C2}r_2 + k_{C3}r_3)X - DC - CTR \tag{4e}$$

$$\frac{dV}{dt} = F_{in} \tag{4f}$$

where S_{in} is the substrate concentration in the feed, F_{in} is the inlet feed rate, V is the culture medium volume and D is the dilution rate ($D = F_{in}/V$). OTR and CTR represent respectively the oxygen transfer rate from the gas phase to the liquid phase and the carbon transfer rate from the liquid phase to the gas phase. Classical models of OTR and CTR are given by:

$$OTR = k_La(O_{sat} - O) \tag{5a}$$

$$CTR = k_La(C - C_{sat}) \tag{5b}$$

where k_La is the volumetric transfer coefficient and, O_{sat} and C_{sat} are respectively the dissolved oxygen and carbon dioxide concentrations at saturation.

The optimal operating conditions that maximize the biomass productivity are at the boundary of the two regimes. In these conditions, the fermentation and byproduct oxidation rates are equal to zero and, from (2):

$$r_1 = min(r_S, r_{S_{crit}}) \tag{6a}$$

$$r_2 = max(0, r_S - r_{S_{crit}}) \tag{6b}$$

where

$$r_{S_{crit}} = \frac{r_O}{k_{os}} \tag{7a}$$

$$r_S = \frac{S}{S + K_S} \tag{7b}$$

$$r_O = \mu_O \frac{O}{O + K_O} \frac{K_{iP}}{K_{iP} + P} \tag{7c}$$

the following relations hold:

$$r_1 = r_S = r_{S_{crit}} = \frac{r_O}{k_{os}} \tag{8a}$$

$$r_2 = 0 \tag{8b}$$

Expression (7a) shows that the respiratory capacity has an influence on the critical substrate concentration level. For illustration purposes, Fig.3 shows a simulation of a fed-batch yeast culture where the substrate concentration in the culture medium is regulated around a constant theoretical value $S_{sp} = 0.0226 g/l$. This constant value is based on the assumption that the respiratory capacity would not be influenced by the ethanol level ($r_O = \mu_O \frac{O}{O+K_O}$ so that, following (8a), $r_1 = r_{S_{crit}} = r_S$, $r_2 = 0$ and $S_{sp} = S_{crit}$). As this assumption is not correct in practice, ethanol is produced during the batch, thus inhibiting the respiratory capacity and affecting the optimal glucose level, and the biomass growth rate is lower than expected ($r_O = \mu_O \frac{O}{O+K_O} \frac{K_{iE}}{K_{iE}+E}$ so that, following (6), $r_1 = r_{S_{crit}} < r_S$, $r_2 \neq 0$ and $S_{sp} \neq S_{crit}$). A simple regulation strategy, i.e., a regulation that does not adapt the glucose setpoint according to the respiratory capacity variations, does not allow to avoid the production of ethanol, leading to a poor level of productivity (while, as demonstrated in the following, more than $80\ g/l$ of biomass can be obtained within $30\ h$ with glucose setpoint adaptation, only $30\ g/l$ are obtained in Fig. 3).

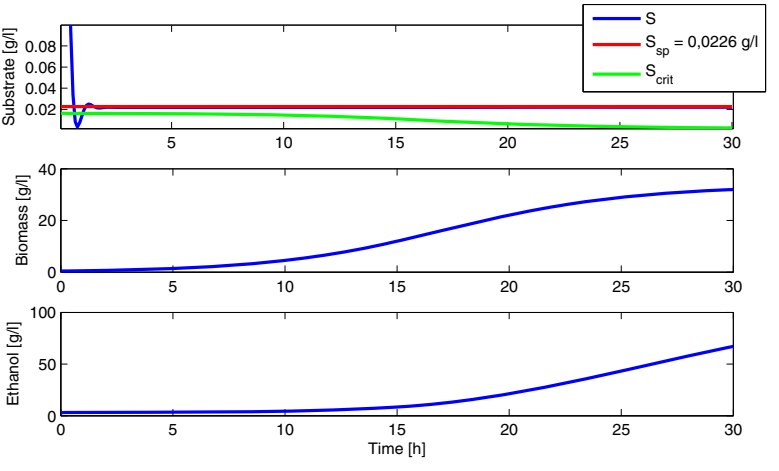

Fig. 3. Simulation of a fed-batch process controlled at a constant S_{sp} value

Consequently, after a trivial mathematical manipulation of (8a) using the Monod law $r_S = \mu_S \frac{S}{S+K_S}$, a relation between the critical substrate concentration level and the cell respiratory capacity is obtained as:

$$S_{crit} = \frac{K_S r_O}{k_{os}\mu_S - r_O} \tag{9}$$

Fig. 4 shows a plot of this relation where the point $[0, 0]$ corresponds to a totally inhibited respiratory capacity, preventing any growth, and the point $[r_{O_{max}}, S_{crit_{max}}]$ corresponds to maximum productivity (i.e. absence of metabolite product in the culture medium and a sufficient level of oxygenation). Obviously, the presence of the byproduct in the culture medium can decrease the respiratory capacity and in turn the value of the critical substrate concentration. Moreover, the estimation of the critical substrate

level S_{crit} requires additional measurements (P, O) and a perfect knowledge of K_S, k_{os}, μ_S, K_O, μ_O and K_{iO}, which are generally uncertain.

In order to maintain the system at the edge between the respirative and respiro-fermentative regimes, it would be necessary to determine on-line an estimation of the biological threshold S_{crit} and to control the substrate concentration in the culture medium around a setpoint S_{sp} ideally equal to S_{crit} in order to reach the optimal operating conditions [7].

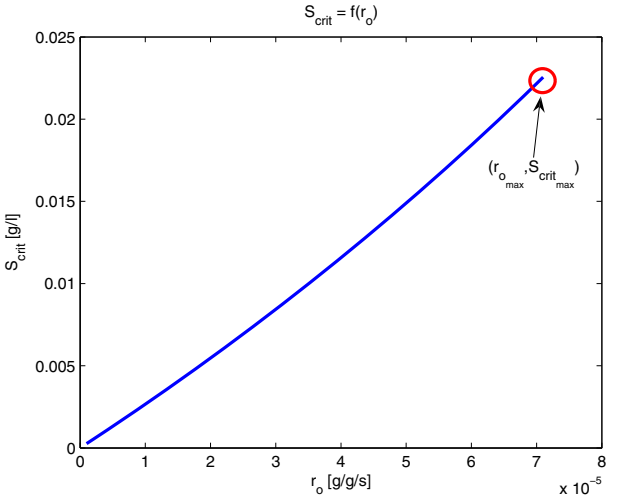

Fig. 4. Critical substrate level (S_{crit}), separating the two regimes, as a function of the respiratory capacity (r_O)

2.2 A Practical Suboptimal Strategy

The maximum of productivity is obtained at the edge between the respirative and respiro-fermentative regimes, where the quantity of by-product is constant and equal to zero ($VP = 0$). Unfortunately, evaluating accurately the volume is a difficult task as it depends on the inlet and outlet flows including F_{in} but also the added base quantity for pH control and several gas flow rates. Moreover, maintaining the quantity of byproduct constant in a fed-batch process means that the byproduct concentration has to decrease while the volume increases. So, even if the volume is correctly measured, VP becomes unmeasurable once P reaches the sensitivity level of the byproduct probe. For those practical limitations, a suboptimal strategy is elaborated through the control of the byproduct concentration around a low value P^* depending on the sensitivity of commercially available probes (for instance, a general order for ethanol probe is $0.1g/l$), and requiring only an estimation of the volume by integration of the feed rate.

The basic principle of the controller is thus to regulate the byproduct at a constant low setpoint, leading to a self-optimizing control in the sense of [14] and ensuring that the culture operates in the respiro-fermentative regime, close to the biological optimum, i.e., close to the edge with the respirative regime.

3 Linearizing Control Strategy

The component-wise mass balances of reaction scheme (1) lead to the following state-space representation

$$\dot{x} = Kr(x)X + Ax - ux + B(u) \tag{10}$$

where $x = [X\ S\ P\ O\ C\ V]'$ is the state vector, $r(x) = [r_1\ r_2\ r_3]'$ is the vector of reaction rates, and $u = D = F_{in}/V$ is the control input (the dilution rate). The matrices K and A, and the vector function $B(\cdot)$ are given by:

$$K = \begin{bmatrix} k_{X1} & k_{X2} & k_{X3} \\ -k_{S1} & -k_{S2} & 0 \\ 0 & k_{P2} & -k_{P3} \\ -k_{O1} & -k_{O2} & -k_{O3} \\ k_{C1} & k_{C2} & k_{C3} \\ 0 & 0 & 0 \end{bmatrix}, \; B(u) = \begin{bmatrix} 0 \\ S_{in}\, u \\ 0 \\ k_L a\, O_{sat} \\ k_L a\, P_{sat} \\ 0 \end{bmatrix}, \tag{11}$$

$$A = \begin{bmatrix} 0_{3\times3} & 0_{3\times2} & 0_{3\times1} \\ 0_{2\times2} & -k_L a\, I_{2\times2} & 0_{2\times2} \\ 0_{1\times3} & 0_{1\times2} & 0 \end{bmatrix},$$

A feedback linearizing controller is illustrated in Figure 5. In a first step, this controller is derived assuming a perfect process knowledge. The basic idea is to derive a nonlinear controller, which allows a linearization of the process behavior ([4,11]).

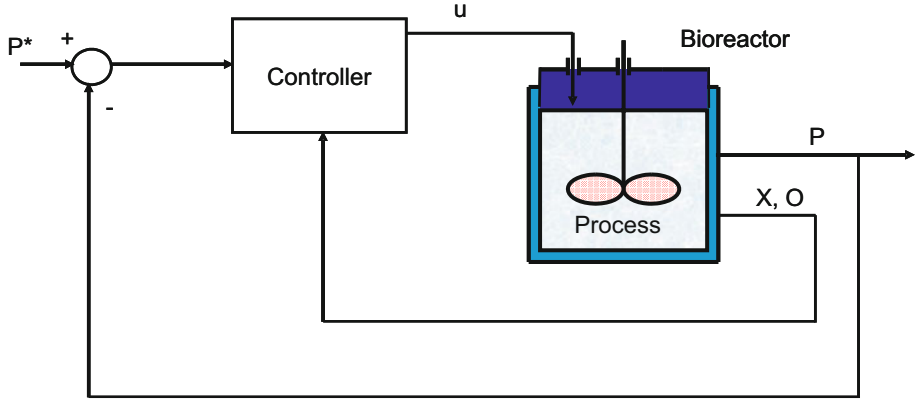

Fig. 5. Linearizing control scheme

As the theoretical value of S_{crit} is very small (below $0.1\ g/l$) and assuming a quasi-steady state of S (i.e. considering that there is no accumulation of glucose when operating the bioreactor in the neighborhood of the optimal operating conditions), the small quantity of substrate VS is almost instantaneously consumed by the cells ($\frac{d(VS)}{dt} \approx 0$ and $S \approx 0$) and (4b) becomes:

$$k_{S2} r_2 X = -k_{S1} r_1 X + S_{in} u \tag{12}$$

where r_1 and r_2 are nonlinear functions of S, P and O as given by (2a-2b).

Replacing $r_2 X$ by (12) in the mass balance equation for P (4c), we obtain:

$$\dot{P} = -\frac{k_{P2} k_{S1}}{k_{S2}} r_1 X - k_{P3} r_3 X - u \left(P - \frac{k_{P2}}{k_{S2}} S_{in} \right) \tag{13}$$

A first-order linear reference model is imposed:

$$\frac{d(P^* - P)}{dt} = -\lambda (P^* - P)\ ,\ \lambda > 0 \tag{14}$$

and a constant setpoint is considered so that:

$$\frac{dP}{dt} = \lambda (P^* - P)\ ,\ \lambda > 0 \tag{15}$$

Equating (15) and (13), the following control law is obtained:

$$F_{in} = V \frac{\lambda (P^* - P) + (\frac{k_{P2} k_{S1}}{k_{S2}} r_1 + k_{P3} r_3) X}{\frac{k_{P2}}{k_{S2}} S_{in} - P} \tag{16}$$

where $\frac{k_{P2} k_{S1}}{k_{S2}} r_1$ and $k_{P3} r_3$, the kinetic expressions, contain several uncertain parameters.

3.1 A Classical Adaptive Strategy

In [4], the parameter uncertainties are handled using an on-line estimation of the kinetic term $\frac{k_{P2} k_{S1}}{k_{S2}} r_1 + k_{P3} r_3$ in the linearizing control law (16).

The main operating assumptions are summarized as follows:

- The byproduct concentration (in this case, ethanol) and the dissolved oxygen and carbon dioxide concentrations are available;
- An exhaust gas analysis (adding 3 new measurements: OTR, CTR and Q_E, the gaseous ethanol outflow rate) is available;
- The stoichiometric parameters are known;
- Kinetics are unknown.

In this earlier work, the biomass is not measured on-line. Nevertheless, nowadays, many biomass probes are readily available and not as expensive as a gas analyzer could be (for instance, a turbidimetric probe or a conductance probe) so that, in this paper, the

biomass concentration measurement X replaces the gas analysis and the dissolved carbon dioxide measurement. Note that in [4], these measurements are used by an asymptotic observer to estimate X. The following adaptive scheme is therefore a simplified version of the original algorithm.

$$F_{in} = V\frac{\lambda(P^* - P) + \hat{\theta}X}{\frac{k_{P2}}{k_{S2}}S_{in} - P} \tag{17}$$

A direct adaptive scheme as described in [2] is used. Consider the following Lyapunov function candidate:

$$V(t) = \frac{1}{2}\left(\tilde{P}^2 + \frac{\tilde{\theta}^2}{\gamma}\right) \tag{18}$$

where $\tilde{P} = P^* - P$, $\tilde{\theta} = \theta - \hat{\theta}$ and γ is a strictly positive scalar. The specific growth rates r_1 and r_3 (and, of course, the pseudo-stoichiometric coefficient k_4) are assumed to be constant so that θ variations are negligible ($\frac{d\theta}{dt} = 0$).

Using the Lyapunov stability theory, the time derivative of the Lyapunov candidate function should be negative for the closed-loop system to be stable:

$$\frac{dV}{dt} = \frac{d\tilde{P}}{dt}\tilde{P} + \tilde{\theta}\frac{d\tilde{\theta}}{dt}\frac{1}{\gamma} \tag{19}$$

Considering (15) and a possible parameter mismatch ($\hat{\theta} \neq \theta$):

$$\frac{d\tilde{P}}{dt} = -\lambda\tilde{P} - \tilde{\theta}X \tag{20}$$

so that (19) becomes:

$$\frac{dV}{dt} = -\lambda\tilde{P}^2 - \tilde{P}\tilde{\theta}X - \tilde{\theta}\frac{d\hat{\theta}}{dt}\frac{1}{\gamma} \tag{21}$$

Choosing the following θ adaptive law cancels the second and the third terms:

$$\frac{d\hat{\theta}}{dt} = \gamma X\tilde{P} \tag{22}$$

Notice that the adaptive law is asymptotically stable as the negativeness of $\frac{dV}{dt}$ in (19) is guaranteed by (22).

3.2 A Robust Strategy

Structural and parametric uncertainties can be lumped into a global parametric error:

$$\delta = \bar{\theta} - \theta \tag{23}$$

where δ is a nonlinear function of (S, P, O) representing possible inexact cancellations of nonlinear terms due to model uncertainties and $\bar{\theta}$ represents the hypothetical exact

unknown value. Rewriting the kinetic term in (17) using the new expression taken from (23), we obtain:

$$u = F_{in} = V\frac{\lambda(P^* - P) + \bar{\theta}X - \delta X}{\frac{k_{P2}}{k_{S2}}S_{in} - P} \tag{24}$$

which corresponds to the perturbed reference system:

$$\dot{P} = \lambda(P^* - P) - \delta X \tag{25}$$

Borrowing the ideas of the *Quasi-LPV* approach [10], we bound the time-varying parameter δ which is supposed to belong to a known set $\Delta := \{\delta : \underline{\delta} \leq \delta \leq \overline{\delta}\}$ with $\underline{\delta}$ and $\overline{\delta}$ respectively representing the minimal and maximal admissible uncertainties.

The parameter λ is designed to ensure some robustness and tracking performance to the overall closed-loop system, which is modeled as follows:

$$\mathcal{M} : \begin{cases} \dot{P} = -\lambda z - \delta X \\ z = P^* - P \end{cases} \tag{26}$$

where $z = P^* - P$ is the performance output.

Let $w = \begin{bmatrix} P^* & X \end{bmatrix}' \subset \mathcal{L}_{2,[0,T]}$ be the disturbance input to the system $\mathcal{M}$, $a(\lambda, \delta) = \begin{bmatrix} \lambda & -\delta \end{bmatrix}$ and $c = \begin{bmatrix} 1 & 0 \end{bmatrix}$. The closed-loop system (26) can be rewritten:

$$\mathcal{M} : \begin{cases} \dot{P} = -\lambda P + a(\lambda, \delta)w \\ z = -P + c\,w\,,\ \delta \in \Delta \end{cases} \tag{27}$$

Consider the finite horizon (for instance, between the instant 0 and the time T) $\mathcal{L}_2$-gain of system $\mathcal{M}$ [9], representing the worst-case of the ratio of $\|z\|_{2,[0,T]}$ (i.e., the finite horizon 2-norm of the tracking error) and $\|w\|_{2,[0,T]}$ (i.e., the finite horizon 2-norm of the disturbance input), which is defined as:

$$\|\mathcal{M}_{wz}\|_{\infty,[0,T]} = \sup_{\delta \in \Delta, 0 \neq w \subset \mathcal{L}_{2,[0,T]}} \frac{\|z\|_{2,[0,T]}}{\|w\|_{2,[0,T]}} \tag{28}$$

Thus, the parameter λ is designed based on the $\mathcal{H}_\infty$ control theory [9,15]. Let $\alpha > 0$ be an upper limiting of $\|\mathcal{M}_{wz}\|_{\infty,[0,T]}$. The problem is to find α such that:

$$\min_{\lambda, \delta \in \Delta} \alpha : \|\mathcal{M}_{wz}\|_{\infty,[0,T]} \leq \alpha \tag{29}$$

while ensuring the robust stability of system (27).

This optimization problem can be written in terms of linear matrix inequalities ($LMIs$) and solved using readily available toolboxes, e.g., SeDuMi [17] can be applied to solve the problem. These constraints can be easily obtained via a quadratic Lyapunov function [3]

$$V(P) = P'QP \tag{30}$$

where Q is a strictly positive symmetric matrix (i.e., $Q = Q' \succ 0$) and " $'$ " corresponds to the transposition matrix operation.

The minimization in (29) is then equivalent to:

$$\min\ \alpha\ :\ V(P) \succ 0\ ,\ \dot{V}(P) + \frac{1}{\alpha} z'z - \alpha w'w \prec 0 \tag{31}$$

where, using (27) and (30), the time derivative of $V(P)$ is given by:

$$\begin{aligned}\dot{V}(P) &= \dot{P}'QP + P'Q\dot{P} \\ &= (-\lambda P + aw)'QP + P'Q(-\lambda P + aw) \\ &= -\lambda P'QP + (aw)'QP - \lambda P'QP + P'Qaw \\ &= -2\lambda P'QP + a'w'QP + P'Qaw \end{aligned} \tag{32}$$

Using (32) in (31), the following expression is obtained:

$$\begin{bmatrix} P \\ w \end{bmatrix}' \begin{bmatrix} -2m & Qa \\ a'Q & -\alpha I_{n_w} \end{bmatrix} \begin{bmatrix} P \\ w \end{bmatrix} - \frac{1}{\alpha} zz' \prec 0 \tag{33}$$

where $m = \lambda Q$ and I_{n_w} is the unity matrix of dimension $n_w \times n_w$ and n_w is the dimension of w.

Now, consider the following lemma (*Schur Complement*):

Lemma 1. The following matrix inequalities are equivalent

$$\begin{aligned} &(i) \quad T > 0, R - ST^{-1}S' \succ 0 \\ &(ii) \quad R > 0, T - S'R^{-1}S \succ 0 \\ &(iii) \quad \begin{bmatrix} R & S \\ S' & T \end{bmatrix} \succ 0 \end{aligned}$$

Hence, using the expression of z, a and c in (27) and Lemma 1, the optimization problem in (29) can be written as follows:

$$\begin{aligned} &\min_{Q,m} \alpha\ :\ \alpha > 0\ ,\ Q = Q' > 0 \text{ and} \\ &\begin{bmatrix} -2m & m & -\delta Q & -1 \\ m & -\alpha & 0 & 1 \\ -\delta Q & 0 & -\alpha & 0 \\ -1 & 1 & 0 & -\alpha \end{bmatrix} \prec 0 \end{aligned} \tag{34}$$

If there exists a feasible solution to the above optimization problem for all δ evaluated at the vertices of Δ, then (29) is satisfied and $\lambda = mQ^{-1}$.

Remark 1: Quadratic Lyapunov functions may be conservative for assessing the stability of parameter-dependent systems [5]. However, a parameter-independent Lyapunov function is considered in this study for two main reasons:

1. λ is parametrized with the Lyapunov matrix Q so as to obtain a convex design condition. A parameter-independent matrix Q therefore results in a parameter-independent control law;
2. the variation of δ is a priori unknown.

Remark 2: This method is likely to be conservative, as the parameter δ has to bound the nonlinearities of the inexactly cancelled terms. Less conservative results can be obtained by considering the approach of [6] to deal with the nonlinearities at the cost of a larger computational effort.

4 Numerical Results

In this section, for comparing the adaptive and robust linearizing control strategies, several numerical simulations considering small-scale bacteria and yeast cultures (respectively in 5 and 20 $[l]$ bioreactors) are performed. The first simulation set is dedicated to yeast cultures with initial and operating conditions: $X_0 = 0.4g/l$, $S_0 = 0.5g/l$, $E_0 = 0.8g/l$, $O_0 = O_{sat} = 0.035g/l$, $C_0 = C_{sat} = 1.286g/l$, $V_0 = 6.8l$, $S_{in} = 350g/l$. The second simulation set is dedicated to bacteria cultures with initial and operating conditions: $X_0 = 0.4g/l$, $S_0 = 0.05g/l$, $A_0 = 0.8g/l$, $O_0 = O_{sat} = 0.035g/l$, $C_0 = C_{sat} = 1.286g/l$, $V_0 = 3.5l$, $S_{in} = 250g/l$.

The values of all model parameters are listed in Tables 1, 2, 3 and 4. Note that, for yeast cultures, coefficients k_{os} and k_{oa} are simply replaced by k_{O1} and k_{03} while $k_{O2} = 0$, in accordance with the model of [16]. For the bacteria model, parameters values are taken from [13] and slightly modified to adapt the yield coefficient normalization to the proposed reaction scheme (1) and kinetic model (with a slight difference in the formulation of r_3).

The state variables are assumed available (i.e., measured) online for feedback. The adaptive and robust linearizing feedback controllers proposed in section 3 aim at tracking the byproduct set-point (E^* and $A^* = 1\ g/l$) which is chosen sufficiently low so as to stay in the neighborhood of the optimal trajectory but also sufficiently high to avoid probe sensitivity limitations. In this setup, a noisy byproduct measurement is considered.

To design the parameter λ in (25) via the optimization problem (29), the parameters K_S, K_P, K_O and K_{i_P}, μ_S, μ_O are assumed to be respectively varying with standard

Table 1. Yield coefficients values of Sonnleitner and Käppeli for *S. cerevisiae* model [16]

Yield coefficients	Values	Units
k_{X1}	0,49	$g\ of\ X/g\ of\ S$
k_{X2}	0,05	$g\ of\ X/g\ of\ S$
k_{X3}	0,72	$g\ of\ X/g\ of\ E$
k_{S1}	1	
k_{S2}	1	
k_{P2}	0,48	$g\ of\ E/g\ of\ S$
k_{P3}	1	
k_{O1}	0,3968	$g\ of\ O_2/g\ of\ S$
k_{O2}	0	$g\ of\ O_2/g\ of\ S$
k_{O3}	1,104	$g\ of\ O_2/g\ of\ E$
k_{C1}	0,5897	$g\ of\ CO_2/g\ of\ S$
k_{C2}	0,4621	$g\ of\ CO_2/g\ of\ S$
k_{C3}	0,6249	$g\ of\ CO_2/g\ of\ E$

Table 2. Kinetic coefficients values of Sonnleitner and Käppeli for the *S. cerevisiae* model [16]

Kinetic coefficients	Values	Units
μ_O	0,256	$g\ of\ O_2/g\ of\ X\ /h$
μ_S	3,5	$g\ of\ S/g\ of\ X\ /h$
K_O	0,0001	$g\ of\ O_2/l$
K_S	0,1	$g\ of\ S/l$
K_E	0,1	$g\ of\ E/l$
K_{iE}	10	$g\ of\ E/l$

Table 3. Yield coefficients values of Rocha's *E.coli* model [13]

Yield coefficients	Values	Units
k_{X1}	1	
k_{X2}	1	
k_{X3}	1	
k_{S1}	0,316	$g\ of\ S/g\ of\ X$
k_{S2}	0,04	$g\ of\ S/g\ of\ X$
k_{P2}	0,157	$g\ of\ A/g\ of\ X$
k_{P3}	0,432	$g\ of\ A/g\ of\ X$
k_{O1}	0,339	$g\ of\ O_2/g\ of\ X$
k_{O2}	0,471	$g\ of\ O_2/g\ of\ X$
k_{O3}	0,955	$g\ of\ O_2/g\ of\ X$
k_{C1}	0,405	$g\ of\ CO_2/g\ of\ X$
k_{C2}	0,754	$g\ of\ CO_2/g\ of\ X$
k_{C3}	1,03	$g\ of\ CO_2/g\ of\ X$
k_{os}	2,02	$g\ of\ O_2/g\ of\ X$
k_{oa}	1,996	$g\ of\ O_2/g\ of\ X$

Table 4. Kinetic coefficients values of Rocha's *E.coli* model [13]

Kinetic coefficients	Values	Units
μ_O	0,7218	$g\ of\ O_2/g\ of\ X\ /h$
μ_S	1,832	$g\ of\ S/g\ of\ X\ /h$
K_O	0,0001	$g\ of\ O_2/l$
K_S	0,1428	$g\ of\ S/l$
K_A	0,5236	$g\ of\ A/l$
K_{iA}	6,952	$g\ of\ A/l$

deviations of 500% and 35% of their nominal values. Simulating the operating conditions of the control strategy in (24), we may infer that $\overline{\delta} = 0.5/3600\ s^{-1}$ and $\underline{\delta} = 0\ s^{-1}$ for yeast cultures and $\overline{\delta} = 0.1/3600\ s^{-1}$ and $\underline{\delta} = 0\ s^{-1}$ for bacteria cultures. In light of (27) and (29), these constraints lead to $\lambda = 0.0056$ and $\lambda = 0.0046$ for yeasts and bacteria, respectively.

Concerning the adaptive control law, $\lambda = 1$ and $\gamma = 0.05$ for yeast cultures while $\lambda = 2$ and $\gamma = 0.25$ for bacteria cultures. Note also that the sampling period is chosen equal to $0.1\ h$.

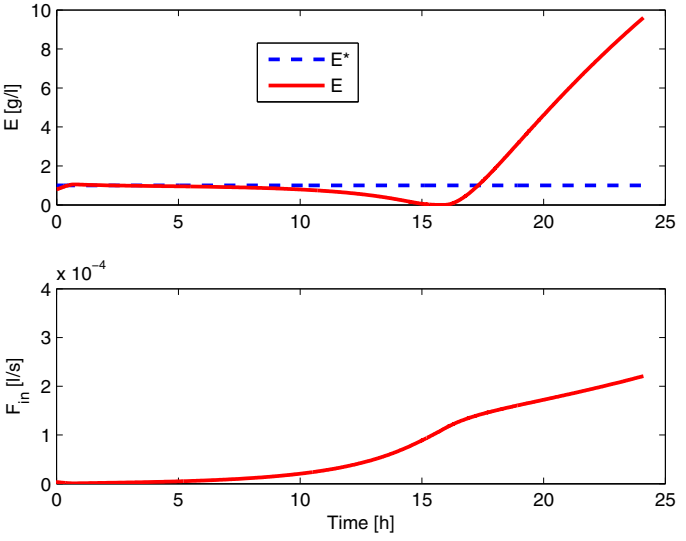

Fig. 6. Yeast cultures – ethanol concentration and feed rate when the controller is designed using a plain linearizing control approach (no adaptation and no robustification) in the presence of modeling errors

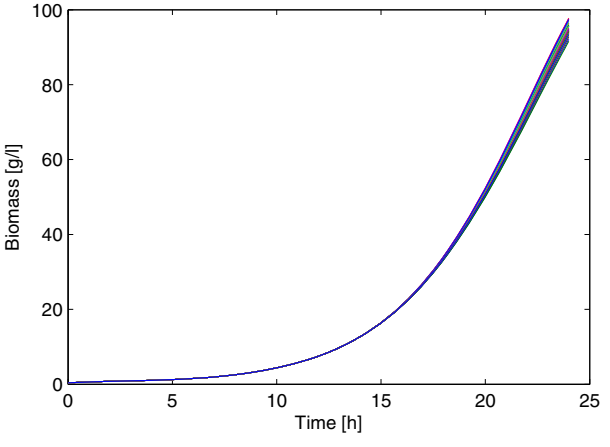

Fig. 7. Yeast cultures – biomass concentrations of 50 runs with random parameter variations and a noise standard deviation of $0.15\ [g/l]$ using the robust control strategy (i.e., $\lambda = 0.0056$)

Before discussing the results of the proposed methods, it is interesting to observe the performance of a plain linearizing controller, i.e. without adaptation or robustification, applied to the yeast process in the presence of modeling errors. For instance, consider the situation where the user selects a relatively high gain $\lambda = 1$, and $\hat{\theta}$ is fixed to $k_{P2}/2$. Figure 6 illustrates the consequences of such choices. Even if the controller behaves correctly during the first hours, the divergence of the ethanol signal during the last hours will impact the quality of the culture.

Figure 7 shows now the closed-loop response of biomass X and figure 8 ethanol E concentrations, for 50 different values of the kinetic parameters (which were randomly chosen) in yeast cultures under a robust control strategy. In all simulation runs, a white noise is added to the ethanol concentration measurement with a standard deviation of $0.15\ [g/l]$ and the culture is considered as always evolving in the optimal operating conditions in which $r_1 = \frac{\mu_O}{k_{O1}}$ and $r_3 = 0$ so that the hypothetical parameter $\bar{\theta}$ in (24) is taken as

$$\bar{\theta} = \frac{k_{P2}\tilde{k}_{S1}}{k_{S2}} r_1 + \tilde{k_{P3}} r_3 \approx \frac{\frac{k_{P2}k_{S1}}{k_{S2}}\mu_O}{k_{O1}} \tag{35}$$

In Figure 7, the different curves are more or less indistinguishable except in the last hours where the consequences of model errors appear. Nevertheless, these results are very satisfactory as model errors have a negligible influence even if, in figure 8, ethanol concentrations may vary from 0.5 to $1.5\ g/l$ when the high biomass dynamics is coupled to important model errors. In order to enhance the idea of a negligible influence of these last variations, figure 9 shows the different productivity levels of each run. It is obvious that, from an operating point of view, the results are satisfactory as the productivity remains higher than $98\ \%$ of the optimal value.

Figures 10 and 11 show the results of a simulation performed with the same initial and operating conditions with the adaptive strategy, in the ideal case where there is no measurement noise, whereas Figures 12 and 13 correspond to a noise standard deviation of $0.05\ [g/l]$ added to the ethanol concentration measurements.

Due to sensitivity problems of the adaptive law, higher noise levels usually lead to computational failures. A way to overcome part of this sensitivty problem is proposed in [4]. The dynamics of ethanol is increasing as the biomass grows, so that the linearizing reference model should take these dynamics into account under the following form:

$$\frac{d(P^* - P)}{dt} = -(\lambda_1 + \lambda_2 X)(P^* - P) \quad \lambda_1, \lambda_2 > 0 \tag{36}$$

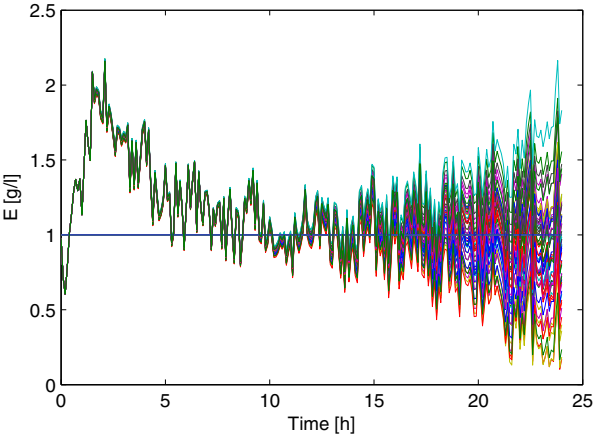

Fig. 8. Yeast cultures – ethanol concentrations of 50 runs with random parameter variations and a noise standard deviation of $0.15\ [g/l]$ using the robust control strategy (i.e., $\lambda = 0.0056$)

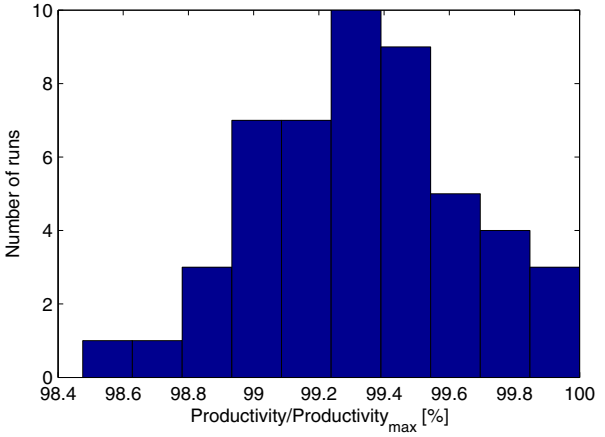

Fig. 9. Yeast cultures – productivity levels of the 50 runs with random parameter variations using the robust control strategy (i.e., $\lambda = 0.0056$)

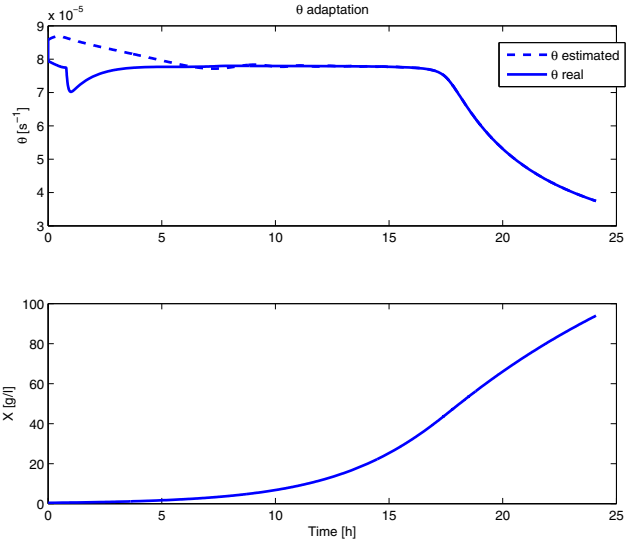

Fig. 10. Yeast cultures – θ adaptation and biomass concentration – adaptive control strategy – no measurement noise

In expression (36), the time constant decreases as the system dynamics (represented by the biomass growth) increases. The new linearizing control law becomes:

$$u = F_{in} = V\frac{(\lambda_1 + \lambda_2 X)(P^* - P) + \theta X}{\frac{k_{P2}}{k_{S2}}S_{in} - P} \tag{37}$$

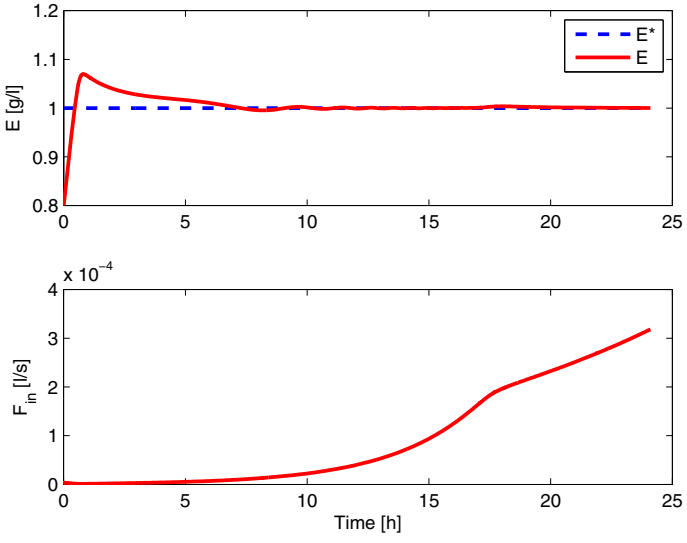

Fig. 11. Yeast cultures – ethanol concentration and feed flow rate – adaptive control strategy – no measurement noise

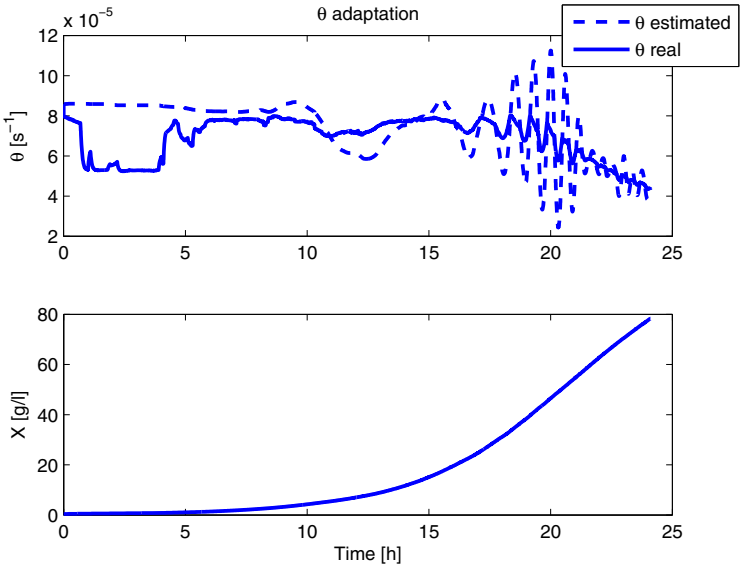

Fig. 12. Yeast cultures – θ adaptation and biomass concentration – adaptive control strategy – noise standard deviation of 0.05 $[g/l]$.

Nevertheless, Figure 14 shows that the adaptive method is still sensitive to the noise level as simulation failures occur for standard deviations higher than $0.125g/l$ (i.e., below the noise level used for the robust strategy).

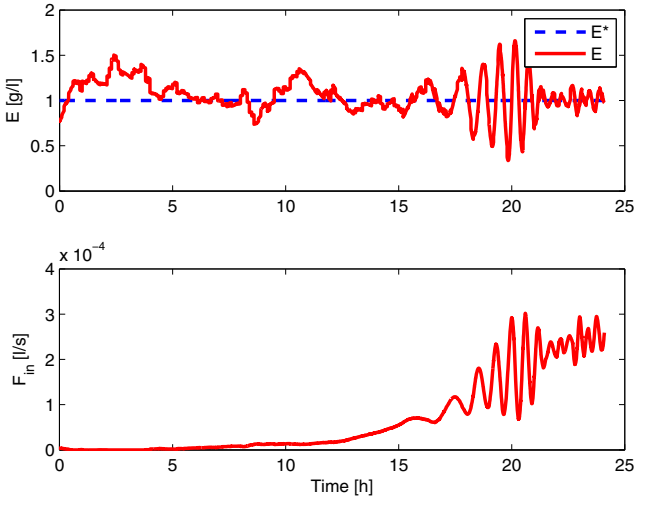

Fig. 13. Yeast cultures – ethanol concentration and feed flow rate – adaptive control strategy – noise standard deviation of 0.05 $[g/l]$

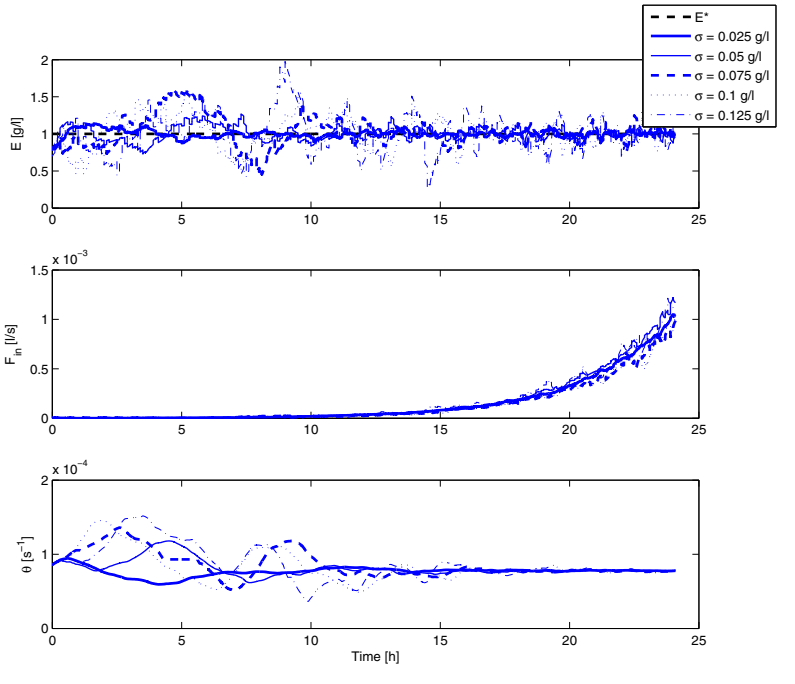

Fig. 14. Yeast cultures – ethanol concentration, feed flow rate and parameter adaptation for 5 different noise levels going from 0.025 to 0.125 g/l. $\lambda_1 = 1$ and $\lambda_2 = 0.2$

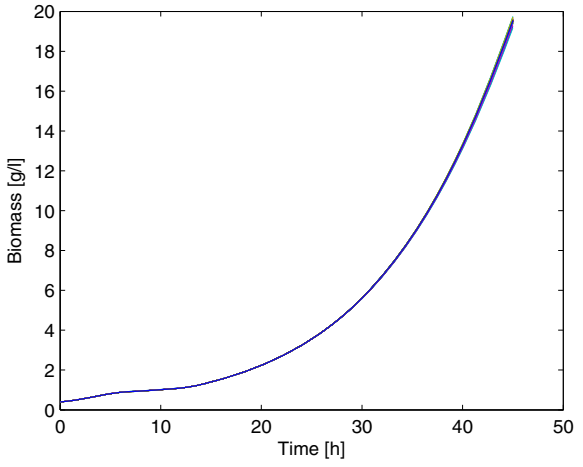

Fig. 15. Bacteria cultures – biomass concentrations of 50 runs with random parameter variations and a noise standard deviation of $0.15\ [g/l]$ using the robust control strategy (i.e., $\lambda = 0.0046$)

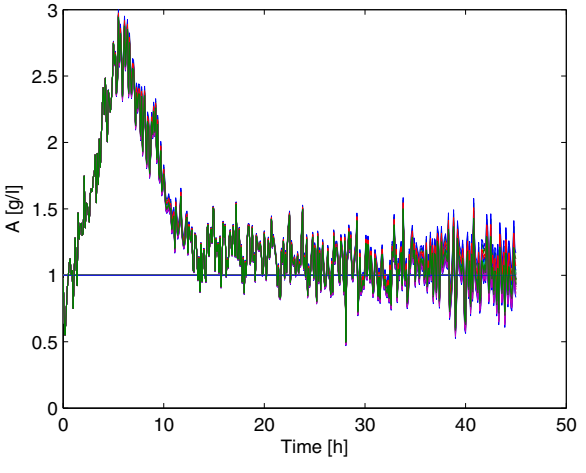

Fig. 16. Bacteria cultures – acetate concentrations of 50 runs with random parameter variations and a noise standard deviation of $0.15\ [g/l]$ using the robust control strategy (i.e., $\lambda = 0.0046$)

However, when the parameter adaptation performs well, the productivity of the adaptive and robust strategies is more or less the same, i.e., a biomass concentration of approximately $90\ g/l$ is obtained within 24 hours.

Figures 15, 16 and 17 show the closed-loop response of biomass X and acetate A concentrations, and the productivity levels for 50 different values of the kinetic parameters which are randomly chosen, in the bacteria cultures under a robust control strategy (noise level of $\sigma = 0.15\ g/l$).

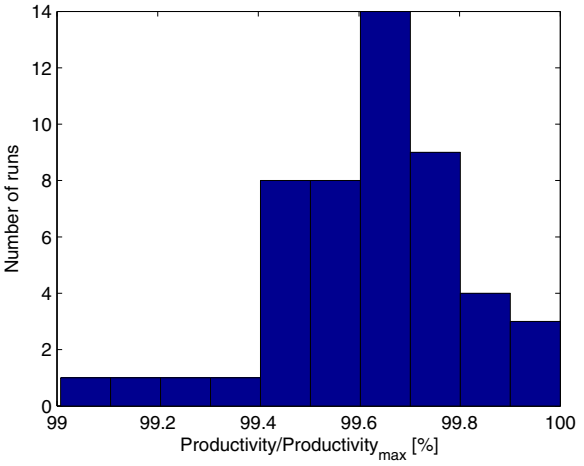

Fig. 17. Bacteria cultures – productivity levels of the 50 runs with random parameter variations using the robust control strategy (i.e., $\lambda = 0.0046$)

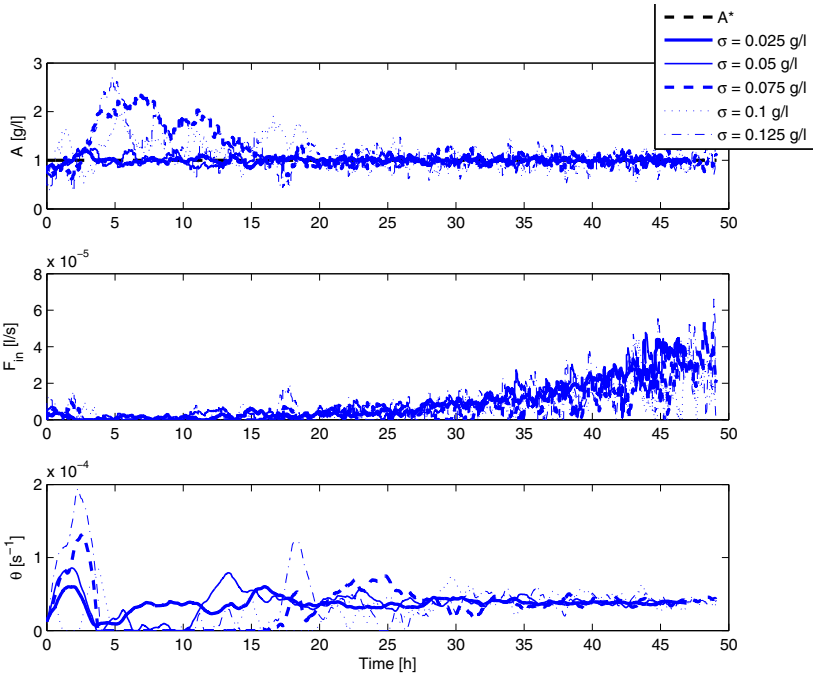

Fig. 18. Bacteria cultures – acetate concentration, feed flow rate and parameter adaptation for 5 different noise levels going from 0.025 to 0.125 g/l. $\lambda_1 = 2$ and $\lambda_2 = 0.4$

Figure 18 show similar simulation runs as in figure 14 with the adaptive strategy where the noise level increases from $\sigma = 0.025$ g/l to $\sigma = 0.125$ g/l. The same comments as in the yeast case concerning the noise sensitivity apply.

Note that, as shown in figure 15, the productivity is lower in the bacteria cultures (for biological and operating reasons, bacteria strains lead to reaction rates and, therefore, growth rates that are smaller than yeast reaction rates). However, from a control point of view, results of the robust strategy are satisfactory in both cases.

5 Conclusions

Linearizing control is a powerful approach to the control of fed-batch bioprocesses. In most applications reported in the literature, on-line parameter adaptation is proposed in order to ensure the control performance despite modeling uncertainties. On-line parameter adaptation is however sensitive to measurement noise, and requires some kind of tuning. On the other hand, robust control provides an easy design procedure, based on well established computational procedures using the LMI formalism. Large parametric and structural uncertainties, as well as measurement noise levels can be dealt with.

References

1. Axelsson, J.P., Mandenius, C.F., Holst, O., Hagander, P., Mattiasson, B.: Experience in using an ethanol sensor to control molasses feed-rates in baker's yeast production. Bioprocess Engineering 3, 1–9 (1988)
2. Bastin, G., Dochain, D.: On-Line Estimation and Adaptive Control of Bioreactors, Process Measurement and Control, vol. 1. Elsevier, Amsterdam (1990)
3. Boyd, S., El-Ghaoui, L., Feron, E., Balakrishnan, V.: Linear Matrix Inequalities in System and Control Theory. SIAM, Philadelphia (1994)
4. Chen, L., Bastin, G., van Breusegem, V.: A case study of adaptive nonlinear regulation of fed-batch biological reactors. Automatica 31(1), 55–65 (1995)
5. Chesi, G., Garulli, A., Tesi, A., Vicino, A.: Robust analysis of lfr systems through homogeneous polynomial lyapunov functions 49(7), 1211–1215 (2004)
6. Coutinho, D., Fu, M., Trofino, A., Danes, P.: L2-gain analysis and control of uncertain nonlinear systems with bounded disturbance inputs. Int'l J. Robust Nonlinear Contr. 18(1), 88–110 (2008)
7. Dewasme, L., Richelle, A., Dehottay, P., Georges, P., Remy, M., Bogaert, P., Vande Wouwer, A.: Linear robust control of s. cerevisiae fed-batch cultures at different scales. Biochemical Engineering Journal (October 2009) (article in press), doi:10.1016/j.bej.2009.10.001
8. Dewasme, L., Vande Wouwer, A., Srinivasan, B., Perrier, M.: Adaptive extremum-seeking control of fed-batch cultures of micro-organisms exhibiting overflow metabolism. In: Proceedings of the ADCHEM Conference in Istanbul, Turkey (July 2009)
9. Green, M., Limebeer, D.: Linear Robust Control. Prentice Hall, Englewood Cliffs (1994)
10. Leith, D., Leithead, W.: Survey of gain-scheduling analysis and design. International Journal of Control 73, 1001–1025 (2000)
11. Pomerleau, Y.: Modélisation et commande d'un procédé fed-batch de culture des levures á pain. Ph.D. thesis, Département de génie chimique. Université de Montréal (1990)
12. Renard, F., Vande Wouwer, A.: Robust adaptive control of yeast fed-batch cultures. Comp. and Chem. Eng. 32, 1238–1248 (2008)
13. Rocha, I.: Model-based strategies for computer-aided operation of recombinant E. coli fermentation. Ph.D. thesis, Universidade do Minho (2003)
14. Skogestad, S.: Control structure design for complete chemical plants. Computers and Chemical Engineering 28(1-2), 219–234 (2004)

15. Skogestad, S., Postlethwaite, I.: Multivariable Feedback Control - Analysis and Design. John Wiley & Sons, New York (2001)
16. Sonnleitner, B., Käppeli, O.: Growth of saccharomyces cerevisiae is controlled by its limited respiratory capacity. Formulation and verification of a hypothesis. Biotechnol. Bioeng. 28, 927–937 (1986)
17. Sturm, J.F., Romanko, O., Pólik, I.: SeDuMi, version 1.1R3 (2006), http://sedumi.mcmaster.ca/
18. Titica, M., Dochain, D., Guay, M.: Adaptive extremum-seeking control of fed-batch bioreactors. European Journal of Control 9(6), 618–631 (2003)